



Study of ISR, FSR, MPI Effects on Inclusive Jet in Pythia and Dire & Study on Madgraph MLM Merging

Natthajuks Pholsen, Chulalongkorn University, Thailand

September 5, 2018

Abstract

In this work, we study the effects of initial state radiation (ISR), final state radiation (FSR), and multiparton interaction (MPI) on the cross section of inclusive jet using CMS_2016_I1459051 analysis. We also demonstrate that to successfully use Madgraph with MLM merging to describe the experimental data, one needs to consider the relevance between x_{qcut} , q_{cut} , and the scale of the process. In doing so, we solve the weird behavior of Madgraph in CMS analyses.

⁰This work could not be accomplished without the help of Armando and other people in Hannes's group. Thank you very much.

Contents

1	Introduction	3
2	Background Knowledge	3
2.1	Quantum Chromodynamics	3
2.2	Jets	4
2.3	Underlying Processes in Monte Carlo Event Generators	4
2.3.1	Hard Process	5
2.3.2	Parton Shower	5
2.3.3	Hadronization	5
2.3.4	Underlying Events	5
2.3.5	Unstable Particle Decays	5
2.4	MC Event Generator and Plugins in This Study	5
2.4.1	Pythia	5
2.4.2	Dire	6
2.4.3	Madgraph	6
2.5	MLM Merging	6
2.6	CMS Analysis for Inclusive Jet Cross Section used in This Study	6
3	Results	7
3.1	Effects of ISR, FSR, MPI on Inclusive Jet Cross Section in Pythia	7
3.1.1	ISR	8
3.1.2	FSR	8
3.1.3	MPI	9
3.1.4	ISR, FSR, and MPI	9
3.2	Effects of ISR, FSR, MPI on Inclusive Jet Cross Section in Dire	10
3.2.1	Background	10
3.2.2	ISR	11
3.2.3	FSR	11
3.2.4	MPI	12
3.2.5	ISR, FSR, MPI	12
3.3	MLM Merging	13
3.3.1	2→3 Matrix Elements	13
3.3.2	Relevance between Xqcut and Qcut	14
3.3.3	Observable Dependence	15
3.3.4	Scale Dependence & CMS Problem Solved	16

1 Introduction

My work in summer student program is divided into two parts. The first part is the study of ISR, FSR, and MPI on the differential cross section of inclusive jet in Pythia and the study of those in Dire. The second part concerns the problem of the weird behavior of Madgraph in CMS analyses.

2 Background Knowledge

2.1 Quantum Chromodynamics

Quantum Chromodynamics (QCD) is a theory that describes strong interactions between partons. Partons is a group of elementary particles including quarks and gluons, which are the exchange particles for strong interaction. The theory is part of the Standard Model (SM) that explains the interactions, namely electromagnetic, weak, and strong interactions, between elementary particles.

Although QCD is very successful, it needs some parameters from the experimental data such as the parton density function (PDF) that explains the composition of quarks and gluons in a particle. Extracting data from experiments for QCD is not an easy task since there is a phenomenon called “confinement.” Confinement means that we can only observe quarks when they form a colorless particle, hadron, which can be divided into two types known as baryon and meson. A baryon is composed of three quarks while a meson is composed of one quark and one antiquark. Confinement happens because the coupling of strong interactions increases when transferred momentum decreases. This means the interactions become stronger when quarks are farther apart. At some point, it will be energetically favorable for the creation of quark-antiquark pairs that bind with original particles to form new hadrons. Hence, this process is called “hadronization.” The process cannot be described by perturbative QCD, and we still do not understand it fully [1].

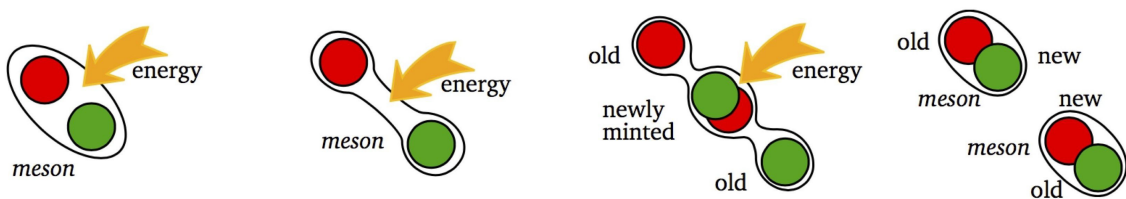


Figure 1: Hadronization Process [7]

2.3.1 Hard Process

The hard process describes the lowest order terms in perturbative QCD. It uses Parton Distribution Functions (PDFs), which are based on experimental data and models, for the probabilistic composition of partons in protons and constructs the core process of each proton-proton collision.

2.3.2 Parton Shower

Similar to electrons radiating photons in Quantum Electrodynamics (QED), partons in QCD also radiate gluons. This is taken into consideration in an MC event generator by a process called parton shower. The process is further divided into the radiation before and after the collision. They are called “initial state radiation (ISR)” and “final state radiation (FSR)” respectively.

2.3.3 Hadronization

Due to the phenomenon of confinement mentioned above, it is impossible to observe separate partons; hence, we need to incorporate hadronization into MC event generators to correctly describe the data from the collisions. The choice of hadronization models is different for each event generator. For example, the string model is used in Pythia while the cluster hadronization model is used in Herwig and Sherpa.

2.3.4 Underlying Events

In one proton-proton collision, there can be more than one parton-parton interaction, and this is often the case because the parton clusters become large at larger energies[4]. The model used to describe events apart from those generated in the hard process is called “multiparton interaction (MPI).” It is implemented differently for each event generator. Moreover, the PDFs also play a role in this part.

2.3.5 Unstable Particle Decays

One more thing to consider after hadronization is that the resulting hadrons may not be stable and decay further. This is taken into account to increase the accuracy of event generators and often referred to as “secondary particle decays.”

Next are information on an event generator, Pythia, and its plugins, Dire and Madgraph, used in this work.

2.4 MC Event Generator and Plugins in This Study

2.4.1 Pythia

Pythia is a general-purpose Monte Carlo event generator that has usually been used in the analyses of particle collisions in high-energy physics. More information on the algorithms of Pythia can be found in Reference [8].

2.4.2 Dire

Dire is available as a plugin to Pythia and Sherpa. It generates parton shower, with next-to-leading-order accuracy, based on the color dipoles and uses transverse momentum in the soft limit as its evolution variable [6].

2.4.3 Madgraph

Madgraph is a matrix-element generator that can be interfaced with parton shower from an MC event generator. It creates matrix elements for events with more than 2 outgoing particles, such as $2 \rightarrow 3$ events. This helps Pythia and other MC event generators that generate only $2 \rightarrow 2$ events.

2.5 MLM Merging

As mentioned that Madgraph, which generates events with more than 2 outgoing particles, is only a plugin, MC event generators can describe three-jet events or more by themselves. The final state radiation resembles having more outgoing particles and is used to approximate them. With Madgraph plugin, the results would be more accurate since matrix elements for multiple-jet events are considered. However, one needs to be careful not to doubly count the multiple-jet matrix elements and the approximation from the parton shower. This is done by a merging algorithm.

The merging algorithm used in this study is called MLM merging, which is proposed by Michelangelo L. Mangano [5]. There are two parameters to be considered in this merging scheme, $xqcut$ and $qcut$. Both of them signify the minimal difference between jets. Their exact definition may vary, but it is largely related to the transverse momentum (p_T) of the jets. The $xqcut$ is implemented in the creation of matrix elements in order to avoid soft and collinear divergences. On the other hand, the $qcut$ is used as a merging scale to avoid the double count.

Let us use the analyses of three-jet events as an example to understand the role of $qcut$ in MLM merging scheme. After $2 \rightarrow 2$ and $2 \rightarrow 3$ matrix elements are generated and showered, the $2 \rightarrow 2$ events that are lower than the $qcut$ and the $2 \rightarrow 3$ events that are higher than the $qcut$ will be accepted, and other events are rejected [5]. This is because the approximation from parton shower ($2 \rightarrow 2$ events) is more accurate in low p_T region and $2 \rightarrow 3$ matrix elements are more accurate in high p_T region. One would also see the verification of this statement from this study.

2.6 CMS Analysis for Inclusive Jet Cross Section used in This Study

In this study, the rivet plugin CMS_2016_I1459051 is used. It plots double differential inclusive jet cross section as a function of p_T and rapidity at a center-of-mass energy of 13 TeV. Jets are clustered by anti- k_t algorithm, and jet size of $R=0.4$ (AK4) and $R=0.7$ (AK7) are considered [9].

In the anti- k_t algorithm, one defines the distance between particle i and j as d_{ij} and the distance between particle i and the beam as d_{iB} :

$$d_{ij} = \min(k_{ti}^{2p}, k_{tj}^{2p}) \frac{\Delta_{ij}^2}{R^2} \quad (1)$$

$$\Delta_{ij}^2 = (y_i - y_j)^2 + (\phi_i - \phi_j)^2 \quad (2)$$

$$d_{iB} = k_{ti}^{2p} \quad (3)$$

where k_{ti} is the transverse momentum of particle i , y is rapidity, ϕ is azimuthal angle, and R is the radius parameter. The variable p signifies the jet algorithm being used, and $p=-1$ for the anti- k_t algorithm [3]. Then, after the calculation of all distances, if the minimum distance is that between particle i and particle j , recombine the particles, but if the minimum distance is that between particle i and the beam, the particle is considered a jet. The process is repeated until there is no particle left.

3 Results

3.1 Effects of ISR, FSR, MPI on Inclusive Jet Cross Section in Pythia

In this subsection, the effects of initial state radiation (ISR), final state radiation (FSR), and multiparton interaction (MPI) on inclusive jet are demonstrated by comparing their graphs with the graph acquired without these processes using CMS_2016_I1459051 analysis.

3.1.1 ISR

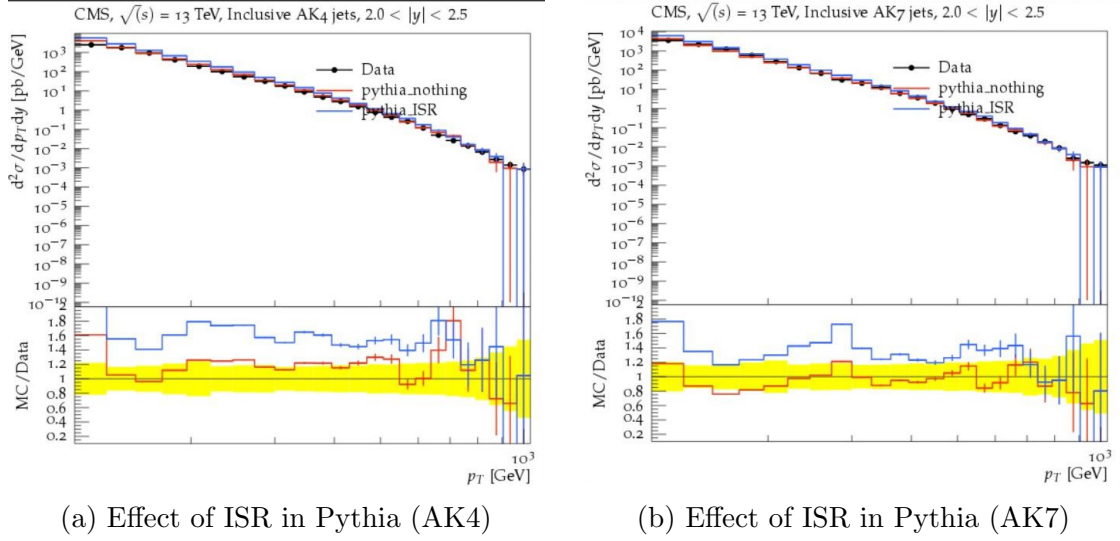


Figure 3: Effect of ISR in Pythia

Initial state radiation increases the differential cross section of inclusive jet by no less than 40% in both AK4 and AK7 jet sizes. This results in too high cross section.

3.1.2 FSR

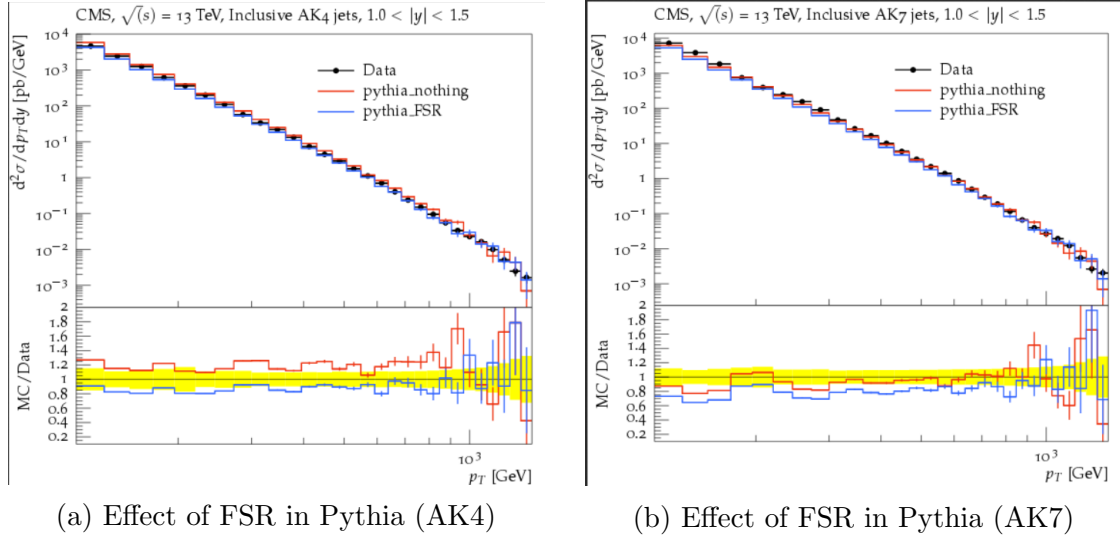


Figure 4: Effect of FSR in Pythia

Final state radiation decreases the differential cross section of inclusive jet by around 30% in AK4 jet size. The effect is less in AK7 than in AK4; hence, it should be concluded that FSR results in radiations that are out of the cone.

3.1.3 MPI

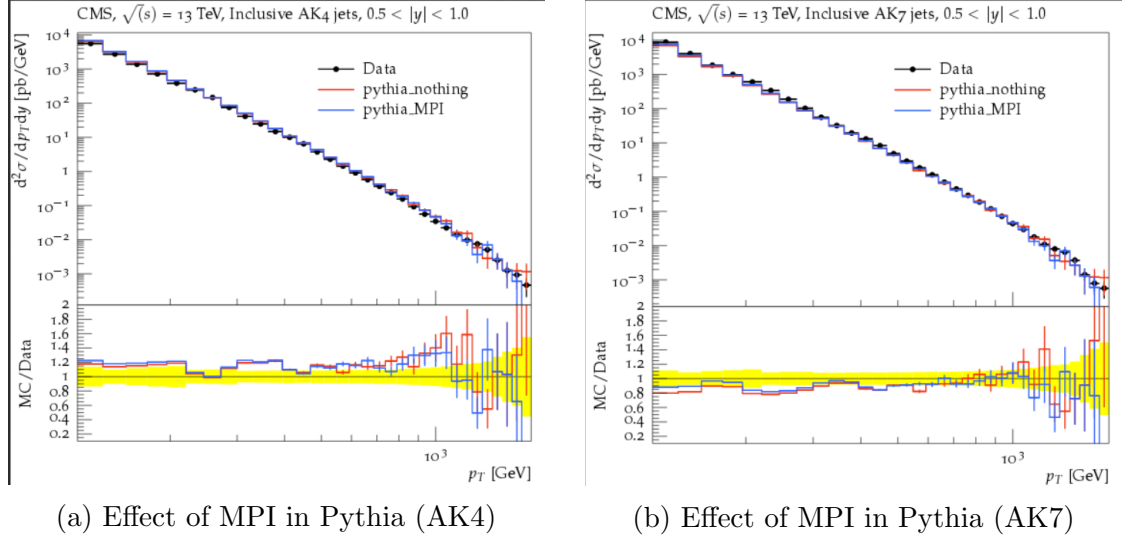


Figure 5: Effect of MPI in Pythia

Multiparton interaction increases a little the differential cross section of inclusive jets. The effect is more distinct in AK7 jet size, which would be because MPI produces more particles which can be clustered into the jet of larger radius.

3.1.4 ISR, FSR, and MPI

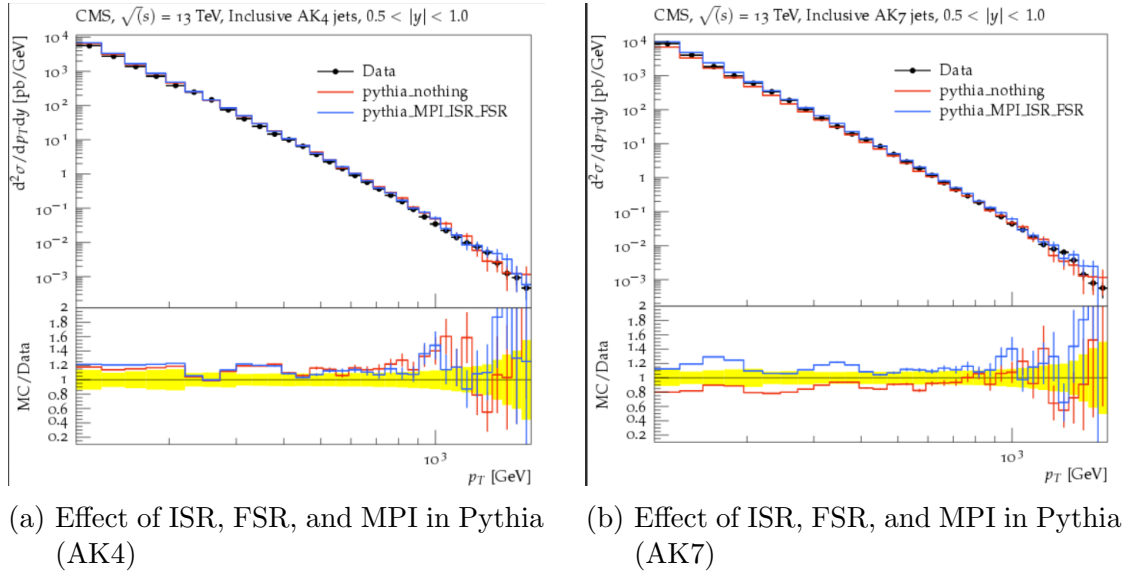


Figure 6: Effect of ISR, FSR, and MPI in Pythia

When the effects of ISR, FSR, and MPI are included altogether, the differential cross section of inclusive jet increases for AK7. The increase is 30% in AK7 compared to much more smaller difference in AK4, and does not contribute to the accuracy of the cross section.

3.2 Effects of ISR, FSR, MPI on Inclusive Jet Cross Section in Dire

In this subsection, ISR and FSR are calculated by Dire as a plugin to Pythia. The effects of Dire on inclusive jet are demonstrated by comparing the graphs obtained with Dire plugin with the graphs produced by Pythia alone using CMS_2016_I1459051 analysis.

3.2.1 Background

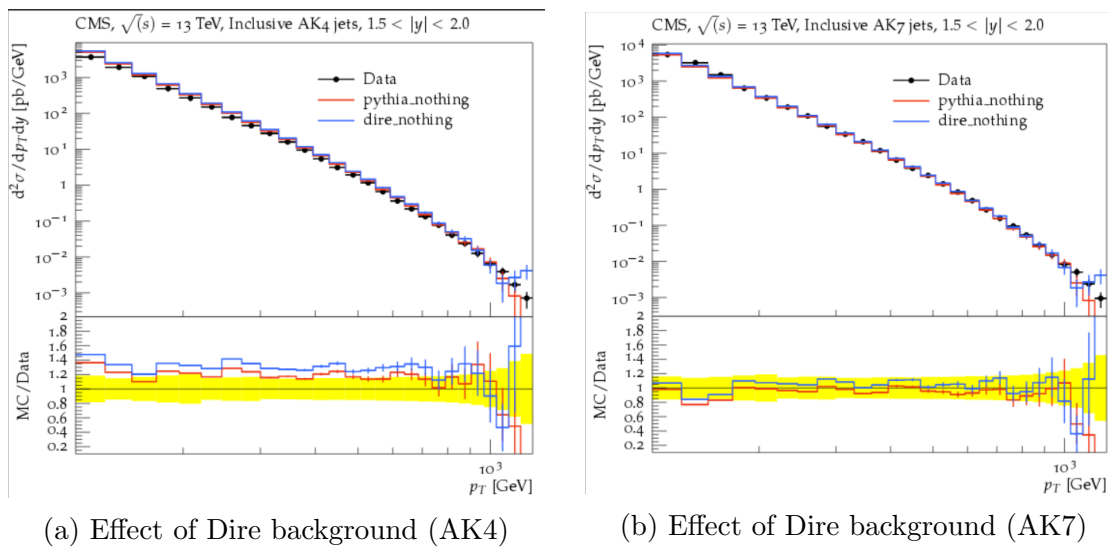


Figure 7: Effect of Dire background

In these graphs, ISR, FSR, and MPI are turned off. It is expected that Dire and Pythia should give the same results since Dire only takes part in ISR and FSR. However, one sees that the differential cross section of inclusive jet from Dire is higher than that from Pythia by 10%. The difference is attributed to different values of α_s in Pythia and Dire.

3.2.2 ISR

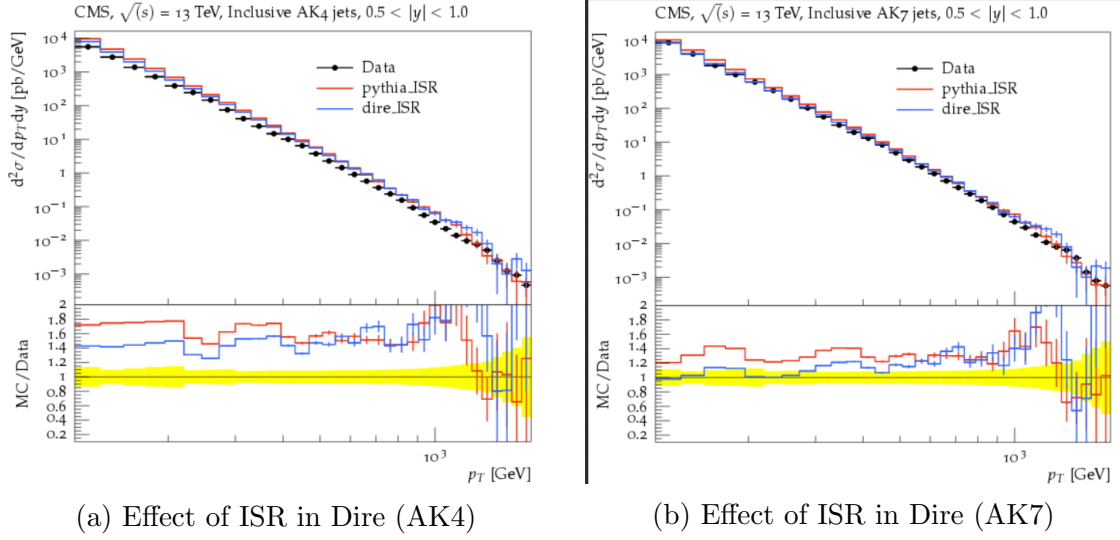


Figure 8: Effect of ISR in Dire

When ISR is turned on, the differential cross section of inclusive jet from Dire is lower than that from Pythia by 20%. This effect dissipates in high p_T region.

3.2.3 FSR

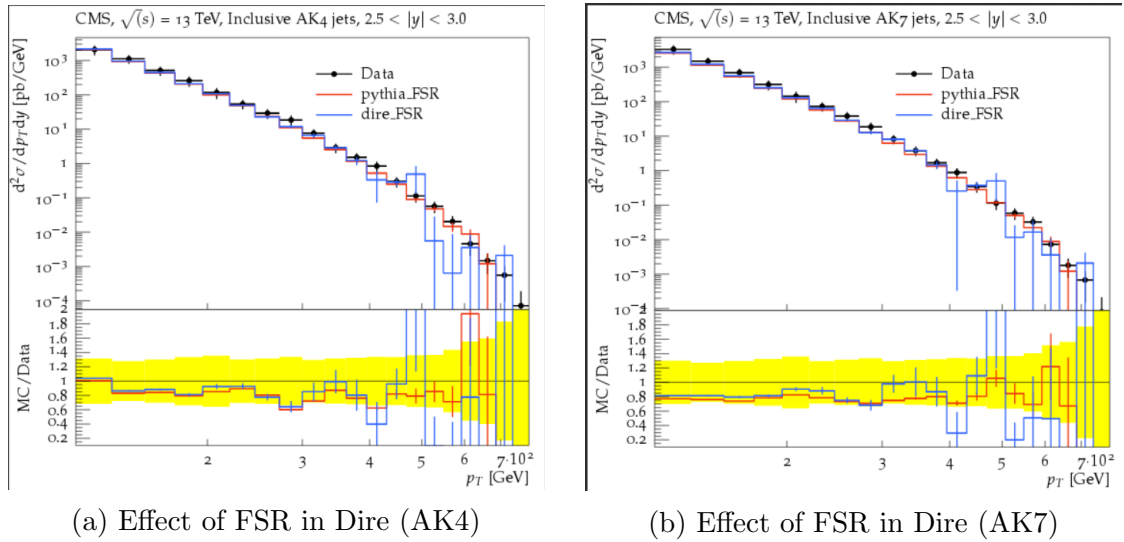
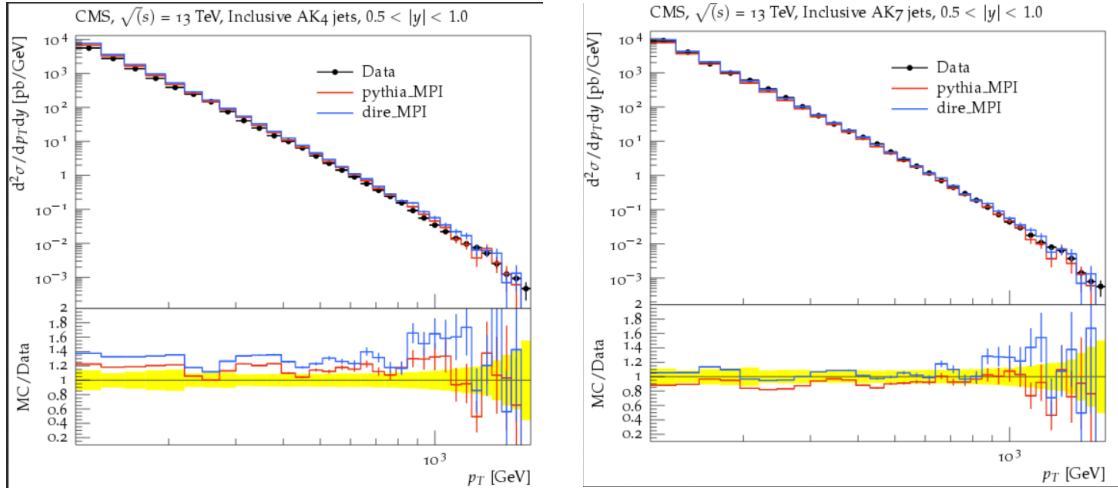


Figure 9: Effect of FSR in Dire

When FSR is turned on, the differential cross section of inclusive jet from Dire is a little higher than that from Pythia.

3.2.4 MPI



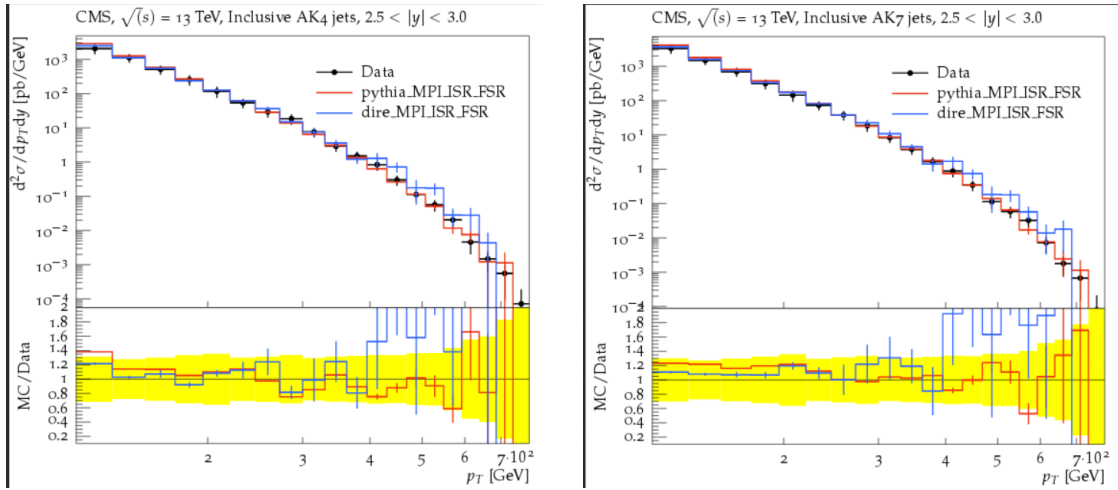
(a) Effect of MPI in Dire (AK4)

(b) Effect of MPI in Dire (AK7)

Figure 10: Effect of MPI in Dire

When MPI is turned on, the differential cross section of inclusive jet from Dire is 20% higher than that from Pythia.

3.2.5 ISR, FSR, MPI



(a) Effect of ISR, FSR, and MPI in Dire (AK4)

(b) Effect of ISR, FSR, and MPI in Dire (AK7)

Figure 11: Effect of ISR, FSR, and MPI in Dire

When ISR, FSR, and MPI are turned on, the differential cross section of inclusive jet from Dire is lower than that from Pythia. From the graphs, it is clear that Dire plugin

helps Pythia to match the data more accurately, but both are within uncertainties.

3.3 MLM Merging

3.3.1 2→3 Matrix Elements

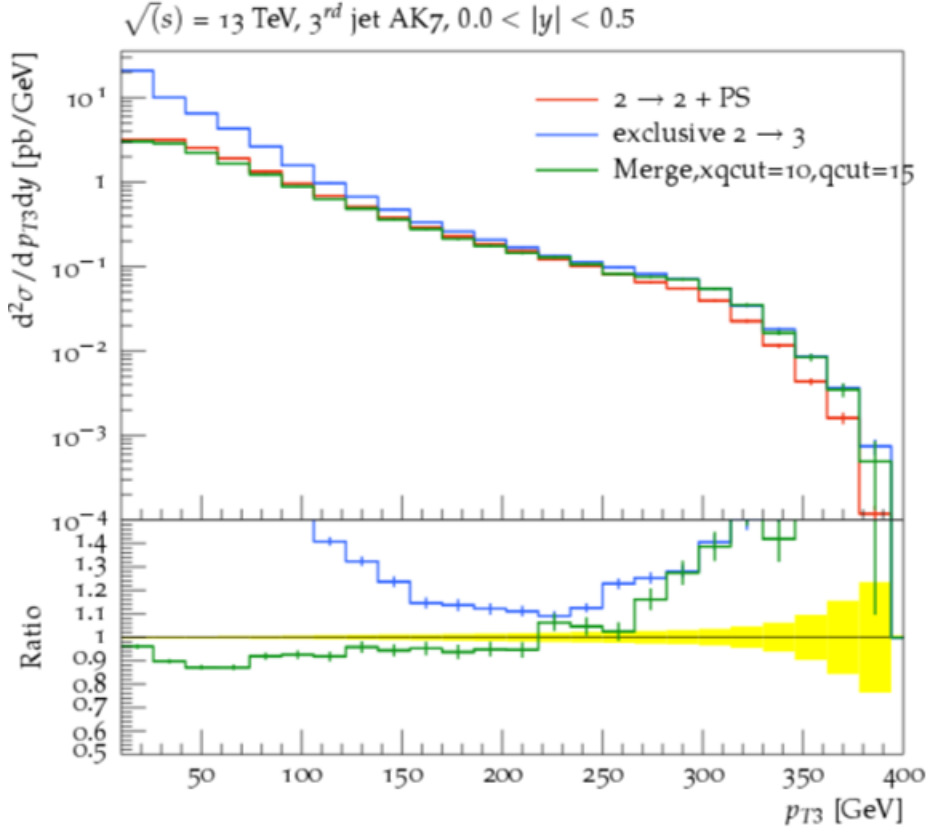


Figure 12: Effect of 2→3 matrix elements

In this graph, the differential cross section is plotted as a function of the p_T of the third jet. The red line is obtained from 2→2 matrix elements with parton shower. The blue line comes from 2→3 matrix elements without parton shower. The green line is the merging between the two with $xqcut$ of 10 GeV and $qcut$ of 15 GeV. It is also required that the p_T of the first jet is between 350 and 400 GeV so that one could see the difference between parton shower and matrix elements clearly.

One would see that in low p_T region the blue line tends to diverge since in this region one also needs to consider interference terms which are better approximated by parton shower. In high p_T region, there is distinct difference between the 2→3 matrix elements and the parton shower. This demonstrates the need to merge the differential cross section from 2→3 matrix elements and parton shower such that one has that from matrix elements in high p_T region and that from parton shower in low p_T region.

3.3.2 Relevance between Xqcut and Qcut

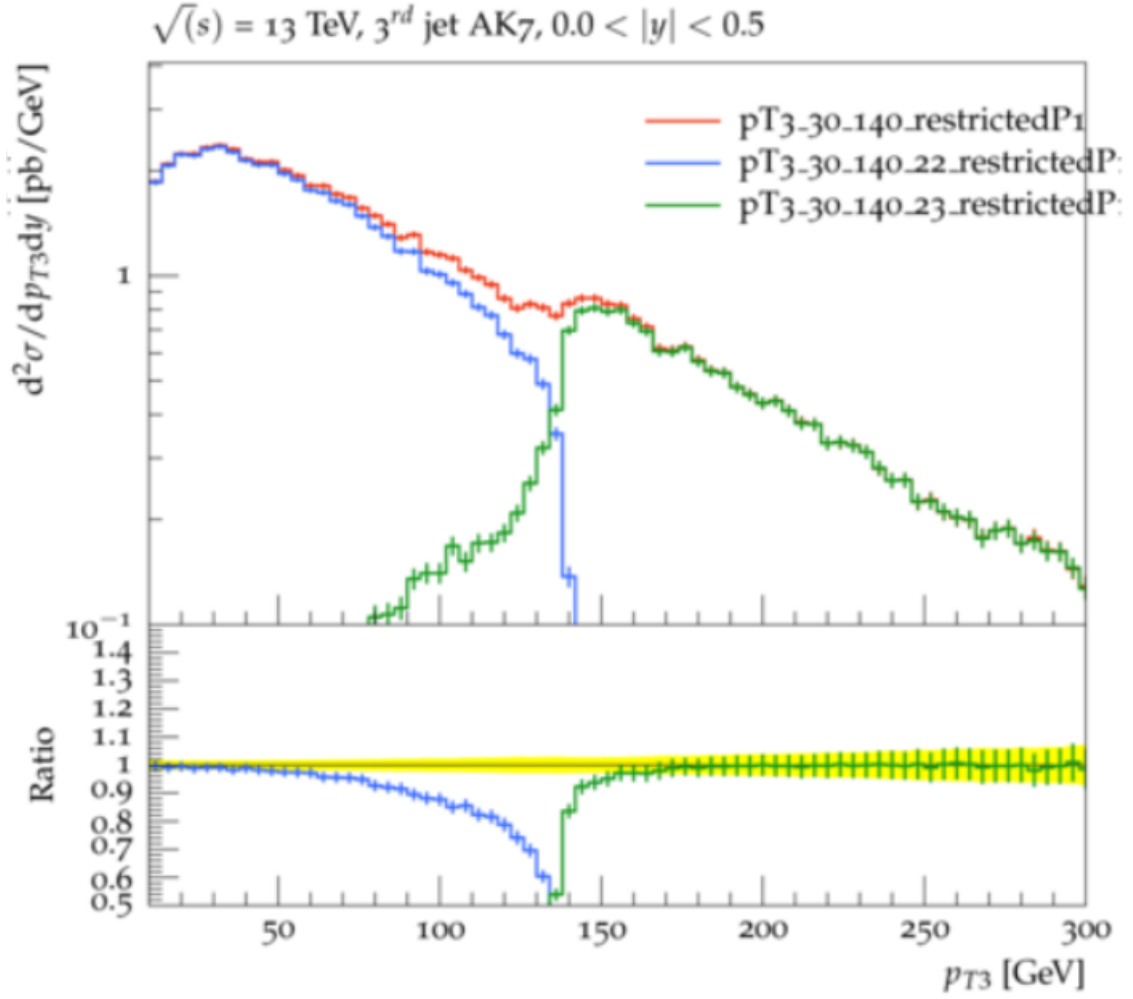


Figure 13: Non-physical graph due to irrelevance in xqcut and qcut

In this graph, the differential cross section is plotted as a function of the p_T of the third jet. The blue line is obtained from $2 \rightarrow 2$ matrix elements while the green line comes from $2 \rightarrow 3$ matrix elements. The red line is the merging between the two. The parton shower, xqcut of 30 GeV, and qcut of 140 GeV are applied in all cases, the p_T of the first jet is between 350 and 400 GeV.

There is a peak at 150 GeV which is non-physical. This happens because the qcut is too far away from the xqcut. Therefore, one must consider the relevance between the xqcut and qcut.

3.3.3 Observable Dependence

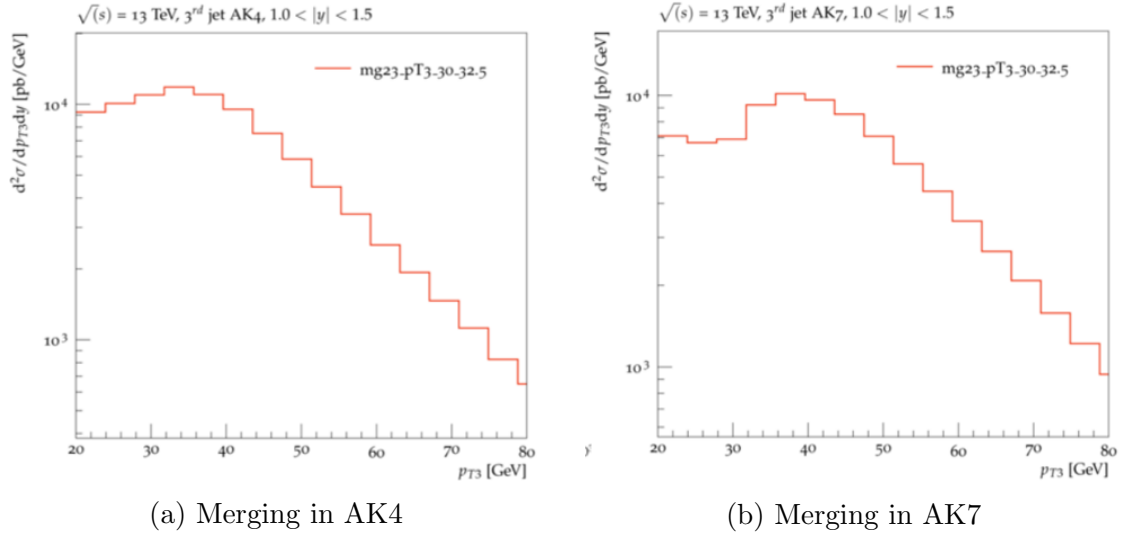


Figure 14: Merging in different jet sizes

The graphs are obtained by merging $2 \rightarrow 2$ and $2 \rightarrow 3$ matrix elements with parton shower for x_{qcut} of 30 GeV and q_{cut} of 32.5 GeV. They plot the differential cross section as a function of the p_T of the third jet.

One would see that the merging is doing fine for AK4. However, there is a large drop in low p_T region in AK7. This shows that suitable x_{qcut} and q_{cut} for the merging depend on observable.

3.3.4 Scale Dependence & CMS Problem Solved

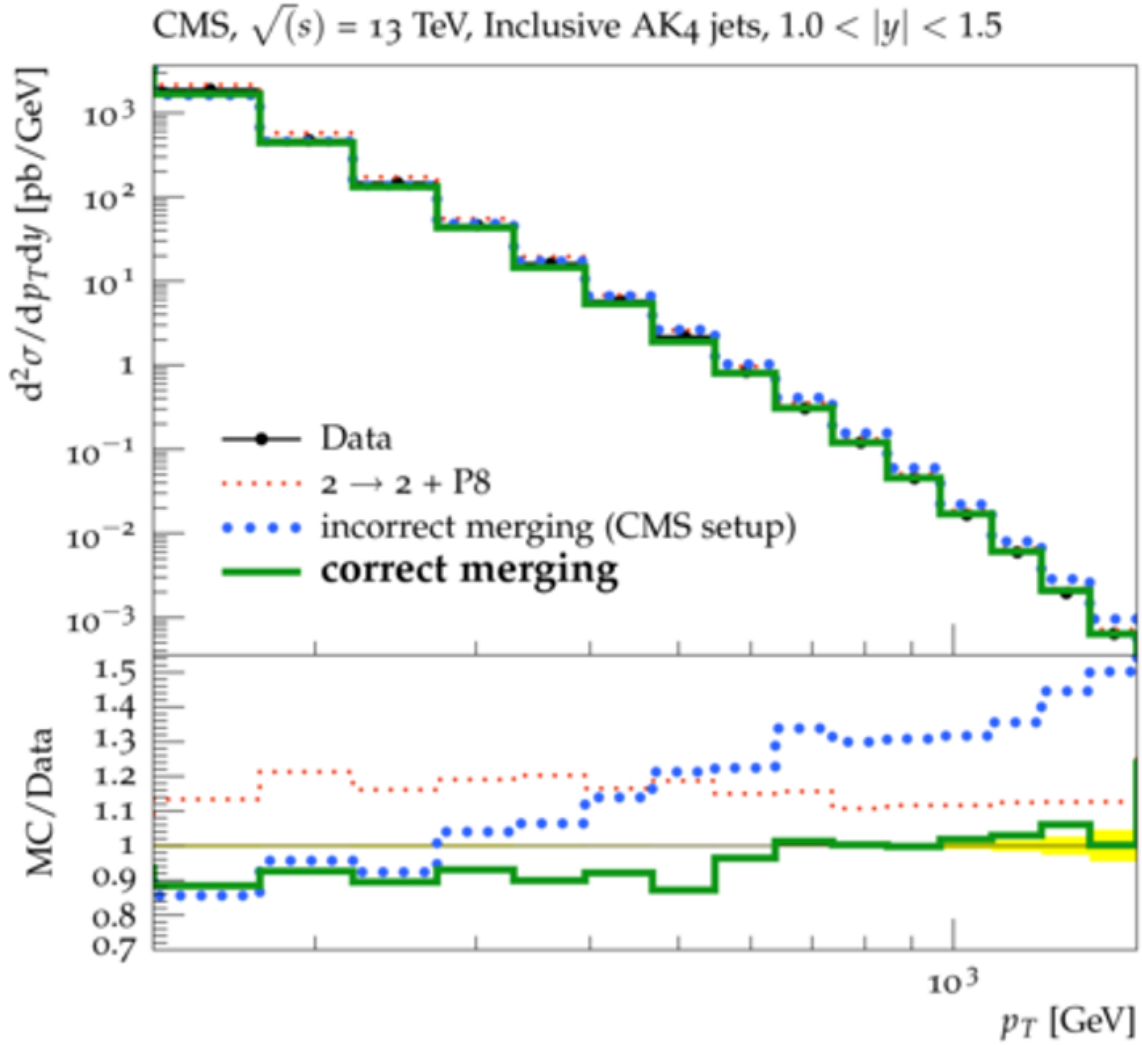


Figure 15: Suitable xqcut and qcut solve the problem in Madgraph and MLM merging

In this graph, the CMS_2016_I1459051 analysis is used to plot the differential cross section as a function of the p_T of inclusive jet. The red line is obtained from $2 \rightarrow 2$ matrix elements with parton shower. The blue line is the merging with xqcut of 10 GeV and qcut of 15 GeV similar to typical CMS setup. The green line is obtained from two sets of data. The first one has H_T , the scalar sum of p_T of every jet in an event, lower than 1,000 GeV with xqcut of 30 GeV and qcut of 50 GeV, and the second one has H_T higher than 1,000 GeV with xqcut of 90 GeV and qcut of 140 GeV.

The merging from the CMS setup does not fit to the data because the xqcut is too far away from the scale of the process. This graph shows that by using suitable xqcut and qcut, one can use Madgraph to describe the data correctly. Hence, the problem stated in Section 1 is solved.

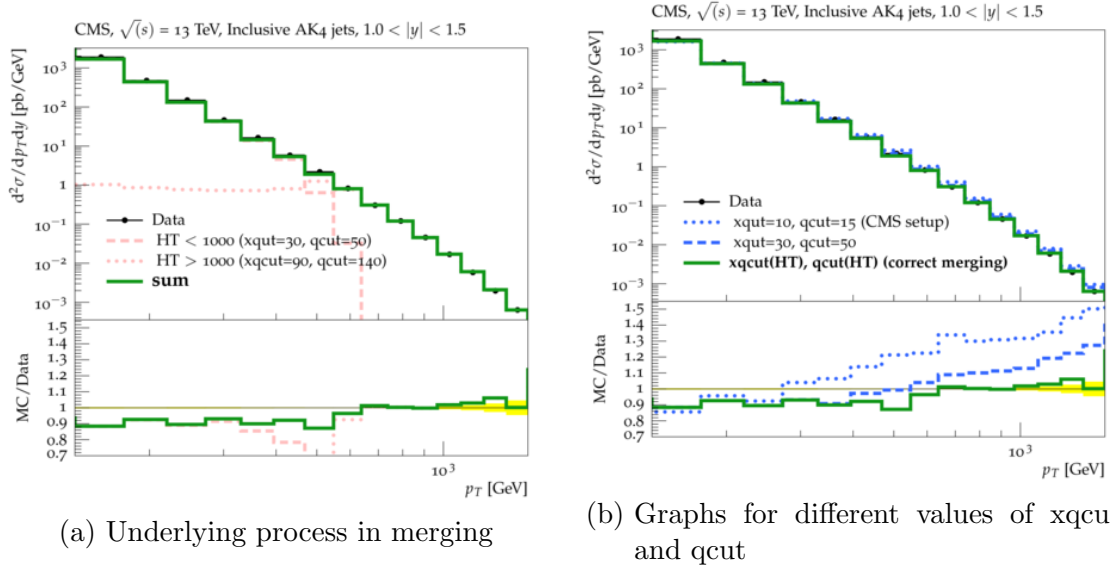


Figure 16: Details in merging

For more details, the graph in Figure 16a shows how the differential cross section in low and high region are filled with events from different restrictions on H_T . Moreover, the graph in Figure 16b shows the differential cross section for different values of $xqcut$ and $qcut$. This strengthens the statement that $xqcut$ and $qcut$ should be the function of the scale of the process (as in the green line.)

References

- [1] A. Ali and G. Kramer, “Jets and QCD: A Historical Review of the Discovery of the Quark and Gluon Jets and its Impact on QCD,” *Eur. Phys. J. H* **36**, 245 (2011) doi:10.1140/epjh/e2011-10047-1 [arXiv:1012.2288 [hep-ph]].
- [2] “CMS homes in on the heaviest quark,” *CERN Courier*, November 27, 2012, <https://cerncourier.com/cms-homes-in-on-the-heaviest-quark/>
- [3] M. Cacciari, G. P. Salam and G. Soyez, “The anti- k_t jet clustering algorithm,” *JHEP* **0804** (2008) 063 doi:10.1088/1126-6708/2008/04/063 [arXiv:0802.1189 [hep-ph]].
- [4] M. H. Seymour and M. Marx, “Monte Carlo Event Generators,” doi:10.1007/978-3-319-05362-2_8 [arXiv:1304.6677 [hep-ph]].
- [5] N. Lavesson and L. Lonnblad, “Merging parton showers and matrix elements: Back to basics,” *JHEP* **0804** (2008) 085 doi:10.1088/1126-6708/2008/04/085 [arXiv:0712.2966 [hep-ph]].
- [6] S. Hche and S. Prestel, “The midpoint between dipole and parton showers,” *Eur. Phys. J. C* **75** (2015) no.9, 461 doi:10.1140/epjc/s10052-015-3684-2 [arXiv:1506.05057 [hep-ph]].
- [7] T. Hubsch, “What is quark confinement?,” *Quora*, October 29, 2017, <https://www.quora.com/What-is-quark-confinement>
- [8] T. Sjöstrand *et al.*, “An Introduction to PYTHIA 8.2,” *Comput. Phys. Commun.* **191** (2015) 159 doi:10.1016/j.cpc.2015.01.024 [arXiv:1410.3012 [hep-ph]].
- [9] V. Khachatryan *et al.* [CMS Collaboration], “Measurement of the double-differential inclusive jet cross section in proton-proton collisions at $\sqrt{s} = 13$ TeV,” *Eur. Phys. J. C* **76** (2016) no.8, 451 doi:10.1140/epjc/s10052-016-4286-3 [arXiv:1605.04436 [hep-ex]].